Journal of Catalysis **185,** 408–414 (1999)
Article ID jcat.1999.2526, available online at http://www.idealibrary.com on IDEAL®

Acylation of 2-Methoxynaphthalene in the Presence of Modified Zeolite HBEA

H. K. Heinichen and W. F. Hölderich[1]

Department of Chemical Technology and Heterogeneous Catalysis, University of Technology RWTH Aachen, Worringerweg 1, 52074 Aachen, Germany

Received December 2, 1998; revised April 6, 1999; accepted April 6, 1999

The influence of postsynthesis treatment such as calcination and acid treatment of zeolite HBEA has been studied in the acylation of 2-methoxynaphthalene with acetic anhydride. The contribution of the inner and outer surface of zeolite HBEA is examined by conversion and product selectivity to a bulky product, which can be formed only on the outer surface of HBEA, and to a linear product, which can be formed on the inner and outer surfaces. Calcination under high heating rate enhances the catalytic activity of the inner surface due to the formation of extraframework alumina species in the micropores. FTIR-adsorption experiments of the bulky probe molecule 2,4,6-tri-*tert*-butylpyridine, which does not fit into the micropores, revealed that these alumina species are located preferentially in the micropores of HBEA. Acid treatment increases the catalytic activity of the outer surface due to the extraction of catalytically active extraframework alumina species out of the micropores and due to the formation of silanol groups, respectively.

Key Words: **acylation; HBEA; 2-methoxynaphthalene; FTIR; adsorption; 2,4,6-tri-*tert*-butylpyridine.**

INTRODUCTION

The Friedel–Crafts acylation of aromatic compounds is a method of choice for the synthesis of aromatic ketones. They are used as intermediates for the production of fine and pharmaceutical chemicals (1). The conventional homogeneously catalyzed synthesis has known disadvantages (3). Therefore, an environmentally benign process is desired. In this context zeolite HBEA showed good catalytic activity in the acylation of anisole (2) and *m*-xylene (3).

We could show (3) that extra framework alumina (EFAL) species formed by calcination under high heating rate are beneficial for the catalytic activity of HBEA in the acylation of *m*-xylene and anisole, respectively. This effect might be due to the migration of catalytically active EFAL species onto the outer surface of HBEA, thereby enhancing the accessibility for the reactants. In order to clarify the location of the EFAL species, now we report on a study of the acylation of 2-methoxynaphthalene (**1**) with acetic anhydride (Fig. 1a) and on FTIR adsorption experiments of the bulky probe molecule 2,4,6-tri-*tert*-butylpyridine (**4**) (Fig. 1b).

During the acylation of 2-methoxynaphthalene with acetic anhydride the linear 6-acetyl-2-methoxynaphthalene (**2**) and the bulky 1-acetyl-2-methoxynaphthalene (**3**) can be formed. Compound **2** can be created at the inner and outer surfaces of zeolite HBEA. Compound **3** is too bulky and cannot enter the micropores (4). Harvey *et al.* (5) reported that 1-acetyl-2-methoxynaphthalene can be formed only on the outer surface of HBEA. The electrophilic attack in the 1- and 6-position of the aromatic ring system is most likely to occur (4). Furthermore, deacylation of 1-acetyl-2-methoxynaphthalene (**3**) was observed in the presence of HBEA (4) (Fig. 1a). Hence, conversion of 2-methoxynaphthalene and product selectivity can be taken as a measure for the contribution of the inner and outer surface to the catalytic activity (5). It is known that the outer surface of zeolite HBEA can contribute significantly to acylation reactions since it can be up to one-third of the total surface area (5, 6).

Additionally, the use of *tert*-butyl-substituted pyridines as probe molecules is a known technique for the FTIR adsorption (7) on acidic hydroxyl groups of a catalyst surface. At least, the aromatic ring system should interact with the hydroxyl groups and a typical shift of the O–H stretching vibration should be observed (8, 9). Even though other authors report about protonation of these sterically hindered pyridines (10). A coordination onto Lewis acid sites is impossible (8). 2,4,6-Tri-*tert*-butylpyridine (**4**) is chosen as probe molecule because it is too large to enter the micropores of HBEA. Hence, after adsorption of this pyridine (**4**) it should be possible to find out which hydroxyl groups are located on the inner and outer surfaces, respectively. In addition, it is interesting to know whether the EFAL species are located on the outer surface of HBEA.

METHODS

Preparation of Catalysts

The acid form of the β-zeolite (HBEA) was obtained from a commercial catalyst kindly provided by Zeolyst

[1] To whom correspondence should be addressed.

0021-9517/99 $30.00

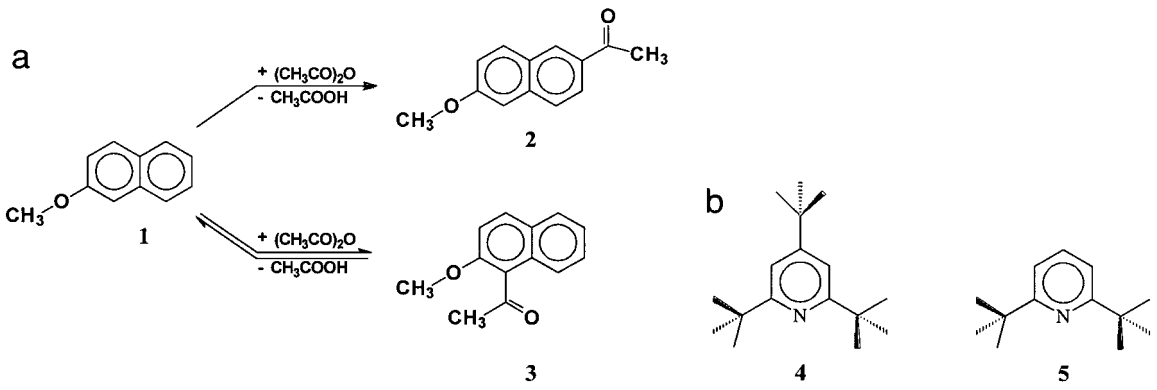

FIG. 1. (a) The acylation of 2-methoxynaphthalene (**1**) to 6-acetyl-2-methoxynaphthalene (**2**) and 1-acetyl-2-methoxynaphthalene (**3**). (b) 2,4,6-Tri-*tert*-butylpyridine (**4**) and 2,6-di-*tert*-butylpyridine (**5**).

(Valfor CP-806-B25). The zeolite was calcined with 1 K/min up to 823 K for 8 h. Subsequent ion exchange was done twice with 2 M aqueous NH_4Cl solution (10 ml/g_{BEA}) at 353 K for 24 h. The zeolite was washed with deionized water, dried at 393 K, and calcined with 1 K/min up to 823 K for 8 h. This sample HBEA1 was the starting material for all the other catalysts.

Subsequent modifications (Table 1) were done by acid treatment (HBEA1-a0.01, HBEA1-a0.1, HBEA1-a1), by calcination under high heating rate (HBEA1-c), and by such a calcination in combination with subsequent acid treatment (HBEA1-c-a0.1). The samples were characterized by ICP-AES, XRD, and nitrogen sorption.

FTIR Adsorption Experiments

FTIR spectroscopy was done with a nicolet 460 Protegé. FTIR spectra of self-supported wafers were recorded between 4000 and 1380 cm^{-1} (hydroxyl and pyridine region). In a typical experiment 10 mg of the zeolite were pressed into a self-supported wafer (13 mm diameter). The wafer was fixed by stainless steel holders and introduced into a vacuum cell. First the wafer was pretreated at 423 K for 30 min and then held at 673 K for 16 h under vacuum (2.5 Pa). After that, the wafer was cooled down to 313 K under vacuum and the first spectra was recorded. Then 2,4,6-tri-*tert*-butylpyridine was allowed to adsorb at 313 K for up to 19 h. The adsorption process lasted such a long time since 2,4,6-tri-*tert*-butylpyridine is solid under these conditions. FTIR spectra were recorded during the course of adsorption. The hydroxyl band associated with extraframework alumina species (3781 cm^{-1}) and the bands associated with the amount of 2,4,6-tri-*tert*-butylpyridine adsorbed were evaluated in relation to the area of the overtone vibration of the T–O–T stretching vibration of the framework (1981 and 1870 cm^{-1}). This area is taken as a kind of internal standard, since it is assumed that this area is a measure for the sample mass reached by the IR-beam. Adsorption experiments with 2,6-di-*tert*-butylpyridine were done correspondingly at an adsorption temperature of 373 K. FTIR measurements of pure 2,4,6-tri-*tert*-butylpyridine and of 2,4,6-tri-*tert*-butylpyridine contacted with HCl, respectively, were performed using a mixture of KBr and the corresponding substance.

TABLE 1

Physicochemical Properties of the HBEA Samples Used in the Acylation of 2-Methoxynaphthalene

HBEA sample	Treatment	Bulk Si/Al	XRD crist.[a] (%)	BET surf. area (m^2/g)	Ext. surf. area (m^2/g)	Micropore vol. (cm^3/g)	Mesopore vol.[b] (cm^3/g)
1	—	15	100	579	200	0.181	0.252
1-a0.01	a.t.[c] 0.01 m/L HCl 298 K 24 h	15	91	566	187	0.181	0.227
1-a0.1	a.t.[c] 0.1 m/L HCl 298 K 24 h	21	93	597	208	0.190	0.254
1-a1	a.t.[c] 1 m/L HCl 298 K 24 h	80	88	591	208	0.187	0.263
1-c	Calc. 12 K/min 1023 K 8 h	15	80	522	188	0.164	0.247
1-c-a0.1	Calc. 12 K/min 1023 K 8 h, a.t.[c] 0.1 m/L HCl 298 K 20 h	20	70	517	187	0.161	0.234

[a] XRD signal $2\Theta = 22.4$.
[b] 2–20 nm BJH.
[c] Acid treated.

Acylation Reaction

The acylation reaction of 2-methoxynaphthalene with acetic anhydride was carried out in the liquid phase in a batch reactor. Sulfolane was used as solvent (25 ml/g catalyst). All chemicals were purchased from Aldrich or Fluka in synthetic quality, dried over a molecular sieve, and used without further purification. Reaction conditions are 373 K, molar ratio of 2-methoxynaphthalene to acetic anhydride of 2, and weight ratio of acetic anhydride to catalyst of 2.5. Liquid samples were taken out of the reactor after 3 and 24 h and analyzed by GC equipped with a RTX 170-1 (30 m) and a FID detector. Conversion is based on the maximal possible conversion of 2-methoxynaphthalene. The selectivity is based on the aromatic compound.

RESULTS AND DISCUSSION

Acylation of 2-Methoxynaphthalene in the Presence of HBEA1, HBEA1-c, and HBEA1-c-a0.1

The conversion and the selectivity in the acylation of 2-methoxynaphthalene are presented in Table 2.

In the presence of HBEA1, 2-methoxynaphthalene is 32% converted after 24 h reaction time. The selectivity to the bulky product 1-acetyl-2-methoxynaphthalene (**3**) is 74% and to the linear product 6-acetyl-2-methoxynaphthalene (**2**) 26%. In this and in all other cases no evidence was found that other products have been formed. The conversion is significantly lower compared to the results of Harvey *et al.* (4), although the selectivity to both products is similar. The high selectivity to **3** indicates that it is formed preferentially on the outer surface. In contrast, the catalytic results obtained over the calcined HBEA1-c are related to two remarkable effects. First, after 24 h the conversion was increased up to 47% and, second, the selectivity to the linear product (**2**) was enhanced up to 61%, whereas the bulky product (**3**) decreased to 39%. Hence, a change in the catalytic activity of the inner and outer surface, respectively, took place. Generally, there are two possible explanations for these findings. Either the catalytic activity on the outer surface was reduced and less bulky product (**3**) could be formed or the activity of the inner surface was increased and more linear product (**2**) was created. N_2-sorption data show (Table 1) that the external surface area as well as the mesopore volume decrease for HBEA1-c. In addition, BET surface and micropore volume decrease due to the loss of crystallinity. However, this change can hardly account for the selectivity change of the two products. The yield of the bulky product (**3**) achieved over HBEA1-c is about 18% and has not changed drastically compared to the yield of 24% obtained over HBEA1. In contrast, the yield for the linear 6-acetyl-2-methoxynaphthalene was increased significantly in the presence of HBEA1-c. Therefore, it can be concluded that the increase in the conversion is due to an increase of the catalytic activity of the inner surface in the micropores of HBEA1-c and that the catalytic activity of the outer surface remained unchanged.

After the acid treatment of HBEA1-c (HBEA1-c-a0.1) a slight decrease of conversion can be observed. However, the product selectivities change again drastically. Now, the formation of the bulky product is again preferred and the selectivity is more or less similar to the selectivity obtained over HBEA1. Once more simple acid treatment has led to a change in the catalytic activity of the inner and outer surface of the sample HBEA1-c-a0.1 compared to HBEA1-c.

The difference in product selectivity observed for HBEA1 and HBEA1-c-a0.1 compared to HBEA1-c can be explained by the extraframework alumina species formed during the calcination process with high heating rate. These EFAL species were already found to be responsible for an activity increase in the acylation of anisole and *m*-xylene with acetic anhydride (3). Hence, the observed increase in conversion for the acylation of 2-methoxynaphthalene can be explained by the amount of extraframework alumina

TABLE 2

Conversion of 2-Methoxynaphthalene (1) and Selectivity to 6-Acetyl-2-methoxynaphthalene (2) and 1-Acetyl-2-methoxynaphthalene (3) in the Acylation of 2-Methoxynaphthalene with Acetic Anhydride in a Batch Reactor after 3 and 24 h

	3 h			24 h		
HBEA sample	Conversion of **1** (%)	Selectivity to **2** (%)	Selectivity to **3** (%)	Conversion of **1** (%)	Selectivity to **2** (%)	Selectivity to **3** (%)
1	30	19	81	32	26	74
1-c	39	53	47	47	61	39
1-c-a0.1	29	23	77	43	31	69
1-a0.01	28	13	87	40	15	85
1-a0.1	53	10	90	46	10	90
1-a1	54	10	90	49	14	86

Note. Reaction conditions: 373 K, *n*-2-methoxynaphthalene/*n*-acetic anhydride = 2, *m*-acetic anhydride/*m*-catalyst = 2.5; solvent: 25 ml sulfolane/g catalyst.

species formed. Furthermore, those species could migrate onto the outer surface of the zeolite as the calcination process becomes more accessible for the reactants. If so, a greater catalytic activity of the outer surface is expected and in consequence, a higher yield of the bulky product should be achieved.

In contrast to the linear 6-acetyl-2-methoxynaphthalene (**2**) the deacylation of the bulky 1-acetyl-2-methoxynaphthalene (**3**) can occur over HBEA (4). Therefore, it might be that the outer surface is catalytically so active that the formed bulky product is very rapidly deacylated. In consequence, the stable linear product is enriched in the reaction mixture and a high selectivity of the linear product could be observed although the extraframework alumina species are located on the outer surface.

On the other hand, if the newly formed extraframework alumina species are preferentially located in the zeolitic micropores of HBEA1-c, this sample would have enhanced catalytic activity in the micropores. This would lead to the observed increase in the selectivity to the linear product (**2**). In addition it would explain the unchanged yield of the bulky product for HBEA1 and HBEA1-c. In summary, the preferential location of the newly formed extraframework alumina species is of interest in order to explain the observed change in product selectivity.

FTIR Adsorption Experiments of 2,4,6-Tri-tert-butylpyridine

In order to evaluate the location of the extraframework alumina species in these catalysts the following consideration was made. Extraframework alumina species show a typical FTIR band at 3781 cm^{-1} in the hydroxyl region (11). This band should disappear when a probe molecule is adsorbed on the hydroxyl groups of the EFAL species. In contrast, EFAL species located in the pores of HBEA should not be affected by such an adsorption if the probe molecule is larger than the pore opening. Then the band at 3781 cm^{-1} should still be visible after the adsorption of the probe molecule. HBEA has a pore opening of 0.76 × 0.64 nm (12). Hence, 2,4,6-tri-*tert*-butylpyridine (**4**) (Fig. 1b) exceeds this pore size because of its bulky *tert*-butyl groups.

Unfortunately, the basic center of 2,4,6-tri-*tert*-butylpyridine at the nitrogen atom is strongly shielded by the two neighbored *tert*-butyl groups. In consequence, the basic center might not be protonated by the Brønsted acid hydroxyl groups. Nevertheless, the interaction of the aromatic ring system of **4** with the Brønsted acidic hydroxyl groups should give a typical shift of about 100 cm^{-1} of the concerning hydroxyl band (9).

Figures 2 and 3 show the spectra in the hydroxyl and pyridine region of the samples HBEA1 and HBEA1-c before and after the adsorption of 2,4,6-tri-*tert*-butylpyridine at 313 K. The spectrum of HBEA1 shows six different types of hydroxyl groups at 3611, 3673, 3735, 3743, and 3782 cm^{-1} as well as a broad band between 3300 and 3700 cm^{-1} (Fig. 2a). The different hydroxyl groups can be attributed as follows (3). The hydroxyl groups at 3611 cm^{-1} are bridging hydroxyls (13), which are directly linked to the aluminum content in the framework. The band at 3673 cm^{-1} is caused by partially attached aluminum to the framework (14). The bands at 3735 cm^{-1} and 3743 cm^{-1} represent internal and external silanol groups (13). Furthermore, the band at 3782 cm^{-1} is caused by hydroxyl groups associated with extraframework

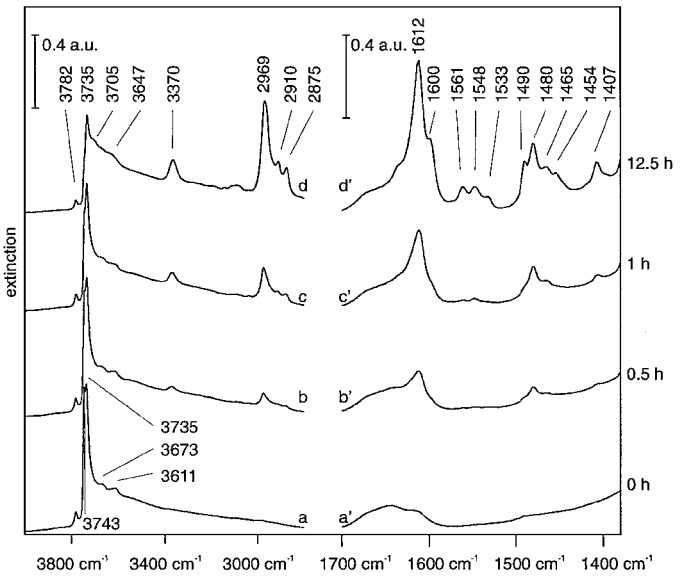

FIG. 2. FTIR spectra in the hydroxyl and framework region of the sample HBEA1 before and after adsorption of 2,4,6-tri-*tert*-butylpyridine at 313 K (0.5, 1, and 12.5 h adsorption time).

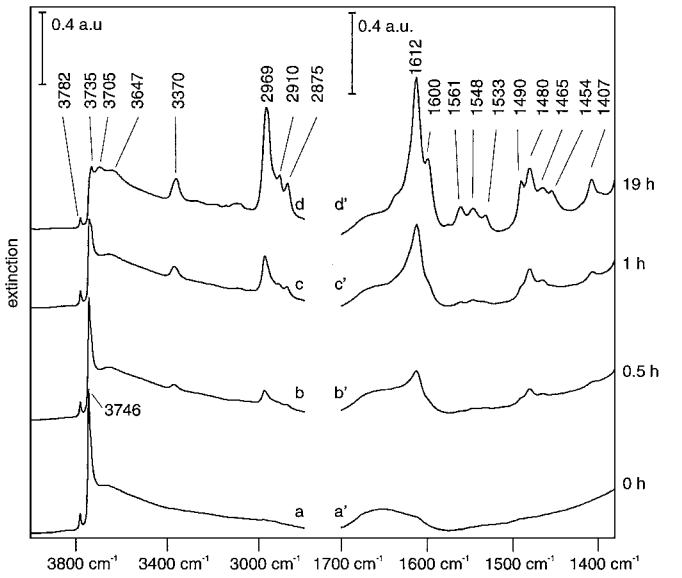

FIG. 3. FTIR spectra in the hydroxyl and framework region of the sample HBEA1-c before and after adsorption of 2,4,6-tri-*tert*-butylpyridine at 313 K (0.5, 1, and 19 h adsorption time).

alumina species (11, 14). Finally, the broad band between 3300 and 3700 cm^{-1} can be associated to very weak or not acidic hydrogen bonded silanol groups (14).

During adsorption of 2,4,6-tri-*tert*-butylpyridine the band at 3743 cm^{-1} disappeared, the bands at 3782 and 3735 cm^{-1} were reduced and new bands arose at 3705, 3647, 3370 cm^{-1}, and in the range of 2900 cm^{-1}. The disappearance of the 3743 cm^{-1} band for external silanol groups indicates that these hydroxyl groups are strongly affected by the adsorption of the bulky probe molecule. The arising band at 3647 cm^{-1} shifted nearly 100 cm^{-1} in comparison to the 3745 cm^{-1}. It shows that at least some of the external silanol groups interact with the aromatic ring system of 2,4,6-tri-*tert*-butylpyridine. A band in the range of 3350 cm^{-1} is typical for a protonated nitrogen atom, indicating that also some nitrogen atoms are protonated. The reason for the appearance of a band at 3705 cm^{-1} is not clear.

In the range of 1700 to 1400 cm^{-1} several new bands appear in the spectrum (Fig. 2d′) at 1612, 1600, 1561, 1533, 1480, 1465, and 1407 cm^{-1} as well as typical bands for pyridine adsorbed on Brønsted and Lewis acid sites at 1548, 1490, and 1454 cm^{-1}. For a better band identification a spectrum of pure 2,4,6-tri-*tert*-butylpyridine had been recorded with the KBr technique (Figs. 4a and 4a′). Comparing this spectrum with the spectrum of HBEA1 (Figs. 2d and 2d′), the bands in the range of 2900 cm^{-1} and the bands at 1600, 1561, and 1407 cm^{-1} can be attributed to the pure 2,4,6-tri-*tert*-butylpyridine. Furthermore, 2,4,6-tri-*tert*-butylpyridine was contacted with gaseous HCl to get protonation of the nitrogen atom and a spectrum was recorded (Figs. 4b and 4b′). This spectrum shows that bands at 1480 and 1465 cm^{-1} can be attributed to protonated 2,4,6-tri-*tert*-butylpyridine. In addition, the spectrum of the protonated 2,4,6-tri-*tert*-butylpyridine showed a similar band for N–H vibration at 3351 cm^{-1} like in the hydroxyl spectrum of HBEA1 (Fig. 2d). In addition the band at 1533 cm^{-1} is typical for 2,6 di-*tert*-butylpyridine (**5**) (Fig. 1b) contacted with HCl (15).

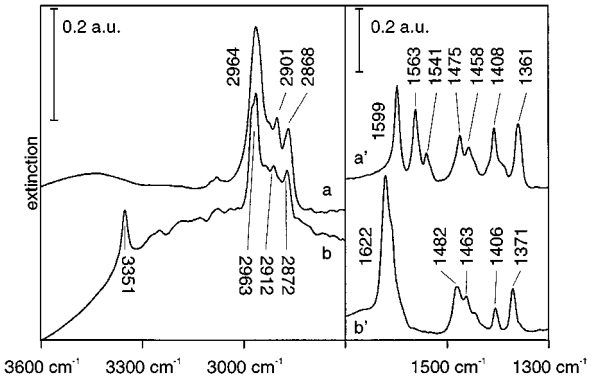

FIG. 4. FTIR spectra in the hydroxyl and pyridine region of pure 2,4,6-tri-*tert*-butylpyridine (a and a′) and of 2,4,6-tri-*tert*-butylpyridine contacted with gaseous HCl (b and b′).

In summary, after the adsorption of 2,4,6-tri-*tert*-butylpyridine on zeolite HBEA1 typical bands appear for 2,4,6-tri-*tert*-butylpyridine and for protonated 2,4,6-tri-*tert*-butylpyridine. This indicates that some 2,4,6-tri-*tert*-butylpyridine molecules are protonated, whereas some interact only with their aromatic ring system with hydroxyl groups. Furthermore, bands appear that are associated with 2,6-di-*tert*-butylpyridine or pyridine. These molecules might be brought into the vacuum cell together with the probe molecule or may have been formed on the zeolite. Indeed, a dealkylation of *tert*-butylbenzene has already been observed during IR adsorption experiments on zeolite HBEA in the literature (16). Therefore, dealkylation of the *tert*-butyl groups on an acidic catalyst might occur.

Unfortunately, pyridine and 2,6-di-*tert*-butylpyridine can adsorb onto hydroxyl groups in the micropores. Thereby, the results of the adsorption of 2,4,6-tri-*tert*-butylpyrdine can be distorted. That is why it is assumed that the dealkylation of 2,4,6-tri-*tert*-butylpyridine had taken place only after a considerable amount of 2,4,6-tri-*tert*-butylpyridine was adsorbed onto the zeolite. However, such a dealkylation reaction can be neglected at the beginning of the adsorption time, i.e., after 0.5 and 1 h.

The band at 3782 cm^{-1} representing the amount of extraframework alumina species not affected by adsorption and the bands around 2900 cm^{-1} representing the amount of 2,4,6-tri-*tert*-butylpyridine adsorbed will be discussed in more detail (Table 3). For the moment we will assume that the EFAL species are equally distributed over the inner and outer surface of the sample HBEA1. A decrease of the band area at 3782 cm^{-1} of about one-third can be expected after adsorption of 2,4,6-tri-*tert*-butylpyridine since the outer surface is considered to be up to 35% of the total surface area of HBEA (5). Furthermore, the hydroxyl groups of the EFAL species are more acidic than the terminal silanol groups. Therefore, the 2,4,6-tri-*tert*-butylpyridine should first adsorb onto the hydroxyl groups of the EFAL species on the outer surface and afterward on the terminal silanol groups.

In contrast to these considerations, a preferential adsorption onto acidic sites other than the hydroxyl groups of the extraframework alumina species can be observed during the first hour (Table 3) in the case of HBEA1. The area of the 3782 cm^{-1} band reduced only around 8% after 0.5 h adsorption time in relation to the reduction after 1 h. On the other hand, at the same time the amount of 2,4,6-tri-*tert*-butylpyridine adsorbed after 0.5 h is already 40% of the amount adsorbed after 1 h. Hence, the first probe molecules adsorbed preferentially not on such hydroxyl groups but on other sites, presumably for the most part terminal silanol groups. One explanation is the preferential location of the extra framework alumina species in the micropores of zeolite HBEA. In that case the adsorption of 2,4,6-tri-*tert*-butylpyridine is not possible and

TABLE 3

Evaluation of the Band Areas of the Hydroxyl Group Associated with Extra Framework Alumina at 3781 cm^{-1} and of the Bands Associated with 2,4,6-Tri-*tert*-butylpyridine (4) at 2900 cm^{-1} after the Adsorption of 4 at the Samples HBEA1 and HBEA-c

HBEA sample	Adsorption time (h)	Band area in relation to the overtone vibration of the framework vibration		Reduction of the total area (%), hydroxyl groups at 3781 cm^{-1}
		Hydroxyl groups at 3781 cm^{-1}	Amount of **4** 2900 cm^{-1}	
1	0.0	0.0204	0.0000	0
	0.5	0.0203	0.1283	0.5
	1.0	0.0192	0.3255	5.9
	12.5	0.0149	1.1177	27.0
1-c	0.0	0.0176	0.0000	0
	0.5	0.0175	0.1292	0.6
	1.0	0.0169	0.3359	4.0
	19.0	0.0117	1.0656	33.5

the probe molecules adsorb preferentially onto the terminal silanol groups. The sample HBEA1-c showed the same preferential adsorption of 2,4,6-tri-*tert*-butylpyridine onto the terminal silanol groups. A second reason can be that the adsorption of 2,4,6-tri-*tert*-butylpyridine on the EFAL species is hindered.

FTIR Adsorption Experiments of 2,6-Di-tert-butylpyridine

In a second experiment 2,6-di-*tert*-butylpyridine (**5**, Fig. 1b) was adsorbed onto the sample HBEA1 and HBEA1-c since that probe molecule fits into the micropores of HBEA. This investigation should disclose whether the band at 3782 cm^{-1} does really disappear when EFAL species are accessible for the probe molecule.

Figure 5 illustrates that only a small shoulder of the 3781 cm^{-1} band remained visible after the adsorption of 2,6-di-*tert*-butylpyridine overnight for HBEA1. It can be concluded that the hydroxyl groups of the EFAL species disappear if a similar, but smaller probe molecule than 2,4,6-tri-*tert*-butylpyridine has access to the micropores. The disappearance of the 3782 cm^{-1} band is not so pronounced in case of HBEA1-c. Nitrogen sorption data shows

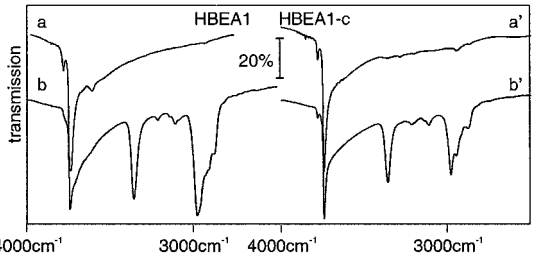

FIG. 5. FTIR spectra in the hydroxyl region of the samples HBEA1 and HBEA1-c before (a and a′) and after (b and b′) the adsorption of 2,6-di-*tert*-butylpyridine at 423 K overnight.

that the micropore volume of HBEA1-c is reduced in comparison to HBEA1 (Table 1). This is caused by the partial framework damage and the larger amount of extraframework alumina species which partially block the pores. So even 2,6-di-*tert*-butylpyridine has no access to all EFAL species. Furthermore, adsorption experiments with pyridine (3) showed the complete disappearance of the 3782 cm^{-1} band for HBEA1-c, indicating that all extraframework alumina species should be accessible for all molecules having similar size like pyridine. In summary, it can be concluded that the extraframework alumina species are located preferentially in the micropores for both samples HBEA1 and HBEA1-c.

Acylation of 2-Methoxynaphthalene in the Presence of HBEA1-a0.01, HBEA1-a0.1, and HBEA1-a1

The acid treated samples HBEA1-a0.01, HBEA1-a0.1, and HBEA1-a1 show the same behavior as the sample HBEA1-c-a0.1 (Table 2). There is an increase in conversion and in the selectivity of the bulky product 1-acetyl-2-methoxynaphthalene with the increase of the concentration of the acid treatment. The N_2-sorption data (Table 1) show only a slight increase in BET and external surface area as well as in micro- and mesopore volume so that the changes in conversion and selectivity cannot be explained by the changes in zeolite texture. Instead, the effect can be explained by the extraction of EFAL species out of the micropores—indicated by the increase in the bulk Si/Al ratio—leading to a decrease of the activity in the micropores. Furthermore, the acid treatment causes the creation of silanol groups as defect sites (3) which might lead to enhanced activity onto the outer surface. After 24 h a drop in conversion can be observed for the samples HBEA1-a0.1 and HBEA1-a1 in comparison to 3 h. For

all other treatments of HBEA1 there was always an increase in 2-methoxynaphthalene acylation after 24 h. This behavior can be explained by significant deacylation of the bulky product 1-acetyl-2-methoxynaphthalene. It indicates again the enhanced catalytic activity on the outer surface since deacylation can take place only outside of the micropores. Additionally, an increase in conversion compared to HBEA1 could be observed after 24 h. This should be due to the more hydrophobic character of the zeolite with increasing Si/Al ratio facilitating the adsorption of the hydrophobic aromatic compound (Table 1).

CONCLUSION

In summary, the adsorption of 2,4,6-tri-*tert*-butylpyridine showed that the main part of the extraframework alumina species are located in the micropores of the samples HBEA1 and HBEA1-c. Hence the increase in the selectivity of the linear product 6-acetyl-2-methoxynaphthalene (**2**) in the presence of HBEA1-c can be explained by the formed EFAL species located in the micropores. In consequence the formation of the bulky product (**3**) is sterically hindered. The bulky product (**3**) is formed on the outer surface of HBEA. In contrary the formation of the linear product 6-acetyl-2-methoxynaphthalene occurs on the inner and outer surfaces. Furthermore, the change in product selectivity after the treatment with acid can be explained by the partial removal of EFAL species out of the micropores of the zeolite. Then, the zeolite loses catalytic activity in the micropores and the formation of the bulky product is preferred.

This results are in line with the observations of Jansen *et al.* (17). These authors discussed that Lewis acid sites are preferentially located in the micropores of HBEA and are due to aluminum atoms partially bonded to the framework. These authors assumed that the band at 3782 cm^{-1} is caused by hydroxyl groups associated with these partially bonded aluminum atoms and not by hydroxyl groups of extraframework alumina species. Nevertheless, whatever is responsible for the band at 3782 cm^{-1}, the corresponding hydroxyl groups are preferentially located in the micropores of zeolite HBEA.

Acid treatment lead to the preferential formation of the bulky product (**3**) due to the extraction of catalytically active extraframework alumina species out of the micropores and maybe also due to the formation of terminal silanol groups.

ACKNOWLEDGMENTS

Financial support of Hoechst Research and Technologies GmbH and Co KG is gratefully acknowledged. The authors express their sincere thanks to Prof. Dr. Klaus Kühlein and Dr. U. Dingerdissen for stimulating discussions.

REFERENCES

1. Kouwenhoven, H. W., and van Bekkum, H., *in* "Handbook of Heterogeneous Catalysis" (G. Ertl, H. Knözinger, and J. Weitkamp, Eds.), p. 2358. VCH, Weinheim, 1997.
2. Smith, K., Zhenhua, Z., Delaude, L., and Hodgson, P. K. G., "Proceedings, 4th International Symposium on Heterog. Catalysis Fine Chemisty." Basel (1996).
3. Heinichen, H. K., Thesis, RWTH-Aachen, 1999.
4. Harvey, G., and Mäder, G., *Collect. Czech. Chem. Commun.* **57**, 862 (1992).
5. Harvey, G., Binder, G., and Prins, R., *Stud. Surf. Sci. Catal.* **94**, 397 (1995).
6. Gaare, K., Akporiaye, D., Holm, K., and Skattebol, L., *Acta Chem. Scand.* **51**, 1229 (1997).
7. Knözinger, H., *in* "Handbook of Heterogeneous Catalysis " (G. Ertl, H. Knözinger, and J. Weitkamp, Eds.), p. 707. VCH, Weinheim, 1997.
8. Knözinger, H., Krietenbrink, H., and Ratnasamy, P., *J. Catal.* **48**, 436 (1977).
9. Su, B. L., and Norberg, V., *Zeolites* **19**, 65 (1997).
10. Dewing, J., Monks, G. T., and Youll, B., *J. Catal.* **44**, 226 (1976).
11. Loeffler, E., Lohse, U., Peuker, Ch., Oehlmann, G., Kustov, L. M., Zholobenko, V. L., and Kazansky, V. B., *Zeolites* **10**, 266 (1990).
12. Meier, W. M., Olson, D. H., and Baerlocher, C., "Atlas of Zeolite Structure Types." Elsevier, London, 1996.
13. Kiricsi, I., Flego, C., Pazzuconi, G., Parker, W. O., Jr., Millini, R., Perego, C., and Bellussi, G., *J. Phys. Chem.* **98**, 4627 (1994).
14. Jia, C., Massiani, P., and Barthomeuf, D., *J. Chem. Soc. Farady Trans.* **89**, 3659 (1993).
15. Matulewicz, E. R. A., Kerkhof, F. P. J., Moulijn, J. A., and Reitsma, H. J., *J. Colloid Interface Sci.* **77**, 110 (1980).
16. Flego, C., Kiricsi, I., Perego, C., and Bellussi, G., *Stud. Surf. Sci. Catal.* **94**, 405 (1995).
17. Jansen, J. C., Creyghton, E. J., Lan Njo, S., van Koningsveld, H., and van Bekkum, H., *Catal. Today* **38**, 205 (1998).